Adaptive Behavior

Adaptive Homing—Robotic Exploration Tours

Verena Vanessa Hafner
Artificial Intelligence Lab, Department of Information Technology, University of Zurich

In this article, a minimalistic model for learning and adaptation of visual homing is presented. Normalized Hebbian learning is used during exploration tours of a mobile robot to learn visual homing and to adapt to the sensory modalities. The sensors of the mobile robot (omnidirectional camera, magnetic compass) have been chosen in a way that their data most closely resemble the sensory data at the disposal of insects such as the desert ant *Cataglyphis* (almost omnidirectional vision, polarized light compass), which is an amazing navigator despite its tiny brain. The learned homing mechanism turned out to be closely related to Lambrinos and colleagues' average landmark vector (ALV) model and is widely independent of any special features of the environment. In contrast to the ALV model or other models of visual homing, feature extraction or landmark segmentation is not necessary. Mobile robot experiments have been performed in an unmodified office environment to test the feasibility of learning of visual homing.

Keywords visual homing · Hebbian learning · mobile robot · insect navigation · snapshot model · ALV model

1 Introduction

In this article, we investigate an interesting aspect of animal behavior, the visual homing strategies of insects. We use a biomimetic approach, called synthetic modeling, combined with mechanisms of adaptation and learning. Such an approach allows us both to transfer biological knowledge to robot technology and to exploit robots to gain insights into biological mechanisms. Visual homing is a navigation strategy usually grouped under the term "guidance" (Trullier, Wiener, Berthoz, & Meyer, 1997): If the goal is not marked by a visible beacon, the goal direction has to be inferred from visual cues of the surrounding scene. Not only insects use guidance as a means of orientation and navigation, but also rodents, as inferred from Morris' water maze experiment (Morris, 1981). Although it is a local navigation strategy, guidance can be used as a building block for more advanced global navigation strategies like topological maps of the environment (Franz, Schölkopf, Mallott, & Bülthoff, 1998b).

A particularly interesting example for the navigation behavior of insects is the desert ant *Cataglyphis*. This animal is an amazing navigator; despite its tiny brain it is able to leave the nest for long distances (up to 200 m) and return to its inconspicuous nest entry. Several theories about its navigation capabilities, at different levels on the navigation hierarchy, have been proposed, ranging from path integration using a polarized light compass (Wehner, 2001; Lambrinos et al., 1997) to visual homing (Collett, 1992) to random search (Müller & Wehner, 1994). The snapshot model (Cartwright & Collett, 1983) explains a possible visual homing strategy, which fits with experimental data of searching behavior in honey bees. The agent stores an omnidirectional snapshot of the environment along the horizon, which is then compared with a snapshot taken at the current position. The compass information has

Correspondence to: V.V. Hafner, Artificial Intelligence Lab, Department of Information Technology, University of Zurich, Winterthurerstr. 190, 8057 Zurich, Switzerland.
E-mail: vhafner@ifi.unizh.ch
Tel: +41-1-6356713, *Fax*: +41-1-6356809

(2001), Vol 9(3–4): 131–141.
[1059–7123 (200110) 9:3-4; 131–141; 028764]

to be used to align the two images according to an external reference direction. The result is a homing vector pointing toward the position where the snapshot was taken. A more parsimonious, parameter-based model has been introduced by Lambrinos et al. (Lambrinos, Möller, Labhart, Pfeifer, & Wehner, 2000), called the average landmark vector (ALV) model. Here, only an average landmark vector has to be stored at the nest, and it is subtracted from the current average landmark vector to calculate the homing vector. In these models, an extraction of the landmarks from the background is required.

It is still unresolved which part of animal navigation strategies is innate, and which part can be acquired through learning and adaptation after birth. Clearly, the underlying ability to learn is innate. In this work, it is assumed that ants learn a visual homing strategy by performing small exploration tours around their nest, always keeping an updated homing vector by using path integration. Here, we will investigate an extremely simple neural structure for learning of visual homing that is widely independent of any special features of the environment. As a means of learning, a normalized version of Hebbian learning is applied, which is described in Section 2. In Section 3, the experimental setup of a mobile robot exploring its environment is introduced. The results are shown in Section 4 and discussed in Section 5, relating them to existing models and strategies of visual homing.

2 Neural Structure and Learning

Within the framework of the snapshot hypothesis (Cartwright & Collett, 1983), successful learning of visual homing results in the association of two scene snapshots, one taken at the nest, and one at the current position of the agent, with a home vector pointing from the current to the nest position. To be able to perform learning, training sets consisting of these three kinds of information pieces have to be created. Ants could accomplish this by performing small exploration tours, always maintaining the home vector by using path integration (Collett & Collett, 2000).

It has been shown that learning of visual homing is in principle possible using a layered neural network structure and backpropagation or delta learning as the learning rule in a self-supervised manner (Hafner & Möller, 2001). It turns out that the learned homing

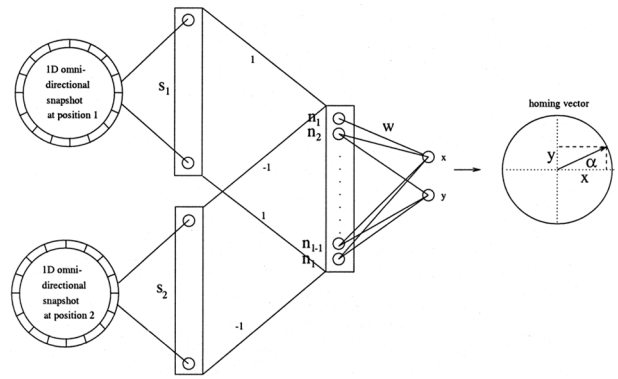

Figure 1 Structural diagram of the neural network model for determining a homing direction from two snapshots. Each snapshot has $l = 90$ ommatidia and is oriented toward an external reference direction. The second snapshot is subtracted from the first one, resulting in l neurons n_i. The weights w_i between n_i and the output layer neurons x and y, which represent the components of the homing vector α, are adjusted using Hebbian learning.

principle when implementing a multi-layer-perceptron (MLP) with up to two hidden layers was functionally the same as when implementing an MLP with just one input layer, consisting of the two snapshots, and one output layer, consisting of the x and y value of the desired homing vector α.

To simplify further the learning, as well as to approach the biological originals, a Hebbian learning rule (Hebb, 1949) is introduced to adapt the weights. The neural structure has been kept as simple as possible, according to the given information (see Figure 1). The intensity values of the snapshot taken at the home position are aligned with respect to an external reference direction and stored. The current snapshot, also being aligned to this direction, is simply subtracted from the home snapshot. Aligning is performed by rotating the current snapshot in a way that it is oriented toward the same direction as is the home snapshot. We chose the number of virtual ommatidia to be 90 since a viewing angle of 4° of one ommatidium is biologically plausible (Zollikofer, Wehner, & Fukushi, 1995). The connections coming from the current snapshot can be seen as "inhibitory" connections. The resulting vector n is directly connected to the home vector (split into its x and y components) via a single layer of weights as can be seen in Figure 1. These connecting weight vectors w_x and w_y adapt online via Hebbian learning during exploration tours.

The change Δw_{ix} in the synaptic weights w_{ix} can be noted as $\Delta w_{ix}(t) = \eta x(t) n_i(t)$, where η is the learning rate, and $n_i(t)$ and $x(t)$ are the activation of two connected neurons at time t. The same holds for Δw_{iy}.

There is strong physiological evidence for Hebbian learning particularly in the hippocampus, the area in the brain of vertebrates that seems to play a role in certain aspects of learning and memory. Long-term potentiation (LTP) is such an effect (for a review see Shors & Matzel, 1997).

To avoid the weights growing infinitely, we use a normalized Hebbian learning rule, in which both weight vectors w_x and w_y that connect the input neurons n_i with x and y, respectively, are normalized. Oja (1982) introduced a convenient form of normalization. In a time-discrete learning rule, normalization is accomplished by

$$w_{ix}(t+1) = \frac{w_{ix}(t) + \eta x(t) n_i(t)}{\sqrt{\sum_j (w_{jx}(t) + \eta x(t) n_j(t))^2}}$$

Assuming that the learning rate η is very small, we can rewrite the equation as a Taylor series of η:

$$w_{ix}(t+1, \eta)$$

$$= w_{ix}(t+1, 0) + \eta \frac{dw_{ix}(t+1, 0)}{d\eta} + O(\eta^2) \quad (1)$$

$$= w_{ix}(t) + \eta x(t)[n_i(t) - x(t) w_{ix}(t)] + O(\eta^2) \quad (2)$$

The term $O(\eta^2)$ can thus be ignored and we get

$$\Delta w_{ix} = \eta x n_i - \eta x^2 w_{ix}, \quad (3)$$

where the second term of Equation 3 can be seen as a regulatory term. The same holds for w_{iy}:

$$\Delta w_{iy} = \eta y n_i - \eta y^2 w_{iy} \quad (4)$$

Instead of directly encoding the two components of the home vector at the output, another possibility of encoding the home vector at the output would be population coding (Georgopoulos, Schwartz, & Kettner, 1986), which is known to be more stable against noise. In this article, however, we only examine direct encoding.

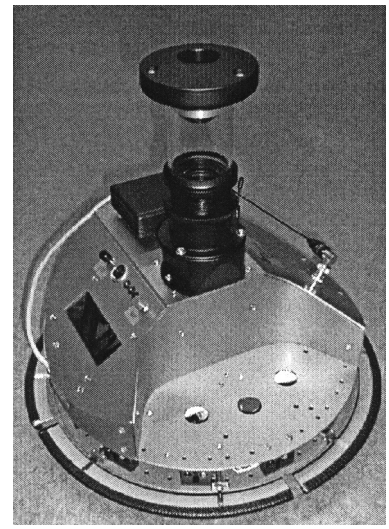

Figure 2 Mobile robot "Samurai," equipped with an omnidirectional camera, a fluxgate magnetic compass, differential steering, and wheel encoders.

3 Experiments

Several experiments have been performed to explore learning of a visual homing strategy and to test this strategy in navigation tasks. The mobile robot "Samurai" (see Figure 2) has been used for these experiments.

3.1 Visual Processing

The mobile robot is equipped with an omnidirectional camera consisting of a USB RoboCAM attached to a convex mirror (Chahl & Srinivasan, 1997). Only the intensity values ("gray values") of this image some degrees above and below the horizon have been used. First, this portion of the camera image has been transformed to its polar mapping and vertically averaged (see Figure 3), resulting in a vector of intensity values. A low pass filter has been applied to the intensity curve to reduce noise, avoid spatial aliasing, and increase robustness. The resulting curve has been shifted by the compass value to get an orientation-invariant place image. The final information available to the artificial neural system is a normalized low-resolution vector (90 virtual ommatidia) of the place image. In our definition, points in the environment corresponding to points in the image are called landmarks. It is therefore possible for a physical object to consist of several landmarks.

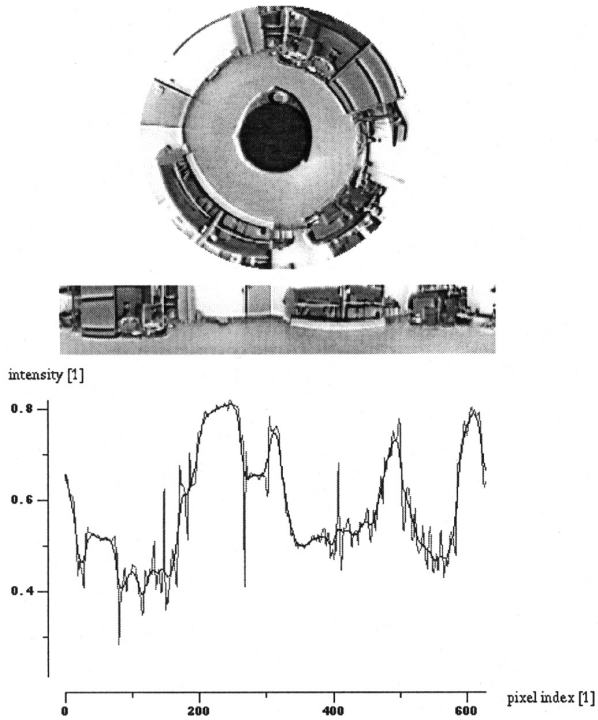

Figure 3 Top: Original camera image taken with the omnidirectional camera on the mobile robot. Center: Polar transform of the original camera image. Only a certain range below and above the horizon is used. Bottom: Intensity curve of the column-averaged image, and its low-pass filtered version.

In previous experiments (not shown here), additional filters have been applied that take the spatial derivative of the snapshots into account. They significantly improved the homing results for one test environment. However, we found out that they were strongly dependent on the specific structure of the environment, that is, the average spatial frequencies. Therefore, we use the lowpass-filtered, normalized one-dimensional image without any further processing.

3.2 Offline Learning Tests

First tests have been performed with off-line learning using a set of camera images that were taken at grid positions in an unmodified office room. We recorded 80 omnidirectional images on an 8×10 grid with a total size of 140×180 cm. Random pairs of images have been fed to the artificial neural network together with the desired output consisting of the vector pointing from one snapshot position in the room to the other. Together with all possible orientations of the robot, the total number of learning samples is $(80^2 - 80) \cdot 90 = 568{,}800$. The results of these tests (see Section 4) showed that the simple neural structure is indeed sufficient to learn visual homing with Hebbian learning and real-world images.

3.3 Mobile Robot Exploration Tours

The next step is the adaptation of the weights during exploration tours of the mobile robot. The robot is equipped with an omnidirectional camera, a compass, differential steering, and wheel encoders as its primary sensors. The compass comprises two fluxgate magnetic field sensors. As the magnetic field is not accurate in buildings, the compass values have been fine-tuned using the camera data. The choice of the sensors is justified by ants having almost omnidirectional vision (Zollikofer et al., 1995), being able to use the polarization pattern of the sky as a compass, and being able to perform path integration (Wehner, 2001).

For the learning task, the robot explores the environment, performing small translations (ca. 80 cm) followed by small rotations (ca. 60°). At the beginning and the end of each translation, an omnidirectional snapshot was taken, together with a compass measurement of the heading direction α. Note that for these exploration tours, we did not use a static home position but defined the first of each pair of snapshots to be the home snapshot. The artificial neural network received the information of the two preprocessed snapshots together with α and adjusted the weights using normalized Hebbian learning as described in Section 2 with exponentially decaying learning rate η. The exploration environment was an unmodified office environment; the accessible ground was of convex shape and flat.

3.4 Robot Homing

After the neural network weights have converged to stable values while the environment is being explored, the robot switched from exploration to homing mode. In this mode, the robot takes a snapshot at an arbitrarily defined home position and is steered to another position by the researcher. The robot then attempts to return to the position where the snapshot has been taken using this snapshot as well as the snapshot taken continuously at the current position. Data from the

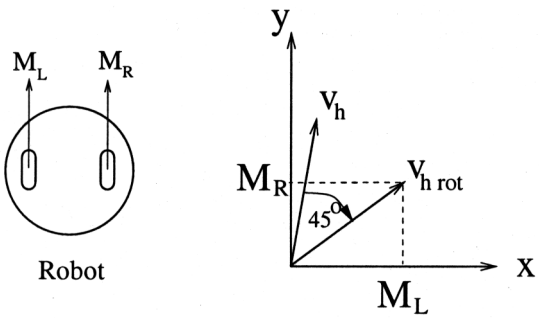

Figure 4 Transformation of the homing vector v_h to motor commands of the mobile robot. The vector is rotated clockwise by 45° to $v_{h\,rot}$; the x component of $v_{h\,rot}$ is used for the left wheel, the y component for the right wheel of the mobile robot.

wheel encoders are not taken into account during the homing procedure. The homing vector v_h is gained from the x and y value of the neural network. $v_h = (x,y) = (\Sigma_i w_{ix} n_i, \Sigma_i w_{iy} n_i)$. To derive the motor values required for moving toward the home position, the homing vector v_h is rotated clockwise by 45° (see Figure 4), and the components are applied to the motors of the robot's wheels (Möller, 2000). The x component of $v_{h\,rot}$ is used for the left wheel, the y component for the right wheel.

$$v_{h_{rot}} = R v_h \begin{pmatrix} \cos\phi & \sin\phi \\ -\sin\phi & \cos\phi \end{pmatrix} v_h, \text{ with } \phi = \frac{\pi}{4} \qquad (5)$$

4 Experimental Results

4.1 Off-line Learning

First we consider the off-line learning experiments with the recorded camera images. After fewer than 1,000 steps of Hebbian learning with exponentially decaying learning rate η ($\eta_0 = 0.035$, $\eta_{t+1} = 0.998\eta_t$), the weights w_x and w_y converged to two sine-shaped curves of different phase shift (see Figure 5). The learning phase finishes when the total weight change becomes considerably small. An explanation of why the weights are converging to this specific form is given in Section 5.1.

The sorted angle errors of 1,000 randomly chosen sets of training data, after the weights have converged using Hebbian learning with the recorded images, can be seen in Figure 6, averaged over 10 runs. The angle error is defined as the absolute angle included from the

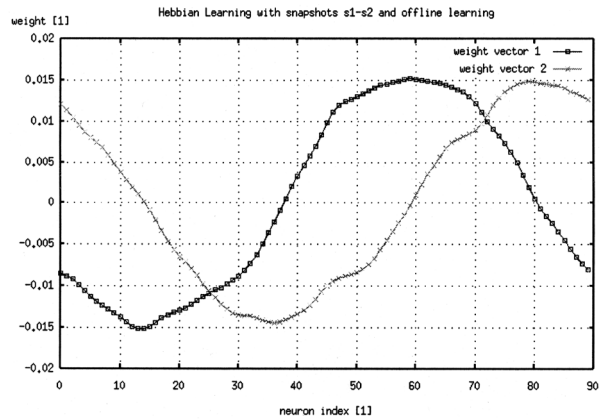

Figure 5 The weight values have converged to shifted sine-shaped curves after 1,000 steps of Hebbian learning with recorded place images.

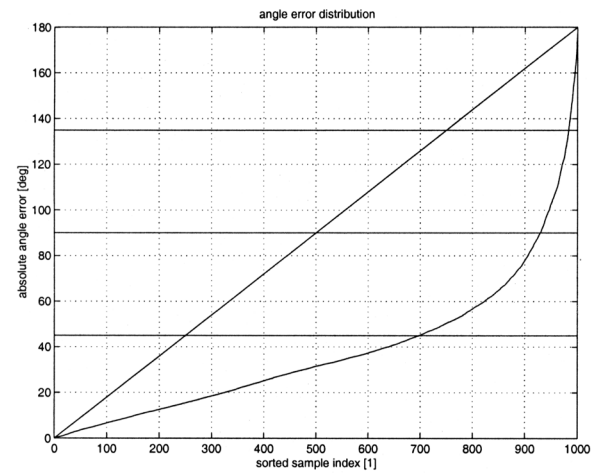

Figure 6 Sorted angle error of 1,000 samples after the weights have converged using Hebbian learning with the recorded images, averaged over 10 runs. The average angle error is smaller than 90° in more than 92% of the test cases; it is smaller than 45° in more than 69% of the test cases.

true homing vector and the homing vector coming from the neural network output. The average angle error is smaller than 90° in more than 92% of the training cases, and smaller than 45° in more than 69% of the training cases. The diagonal line shows the curve for random guesses of the homing vector. Assuming that the errors are equally distributed within the environment positions, the result is converging homing trajectories, since a large percentage of angle errors lie below 90°. If the angle errors were always lying below 90°, the distance to the goal position would decrease

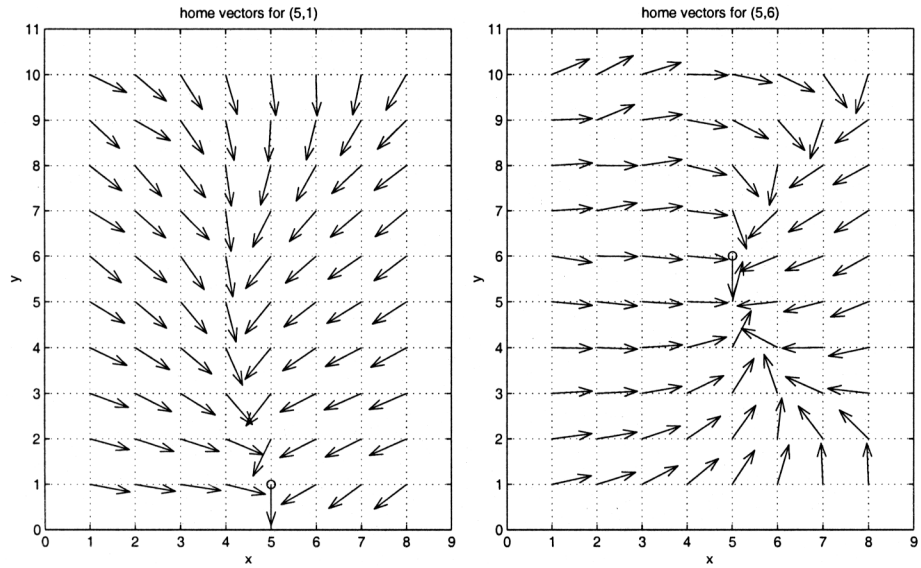

Figure 7 Home vector plots for the set of recorded images after Hebbian learning. The plot on the left shows the home vectors for a snapshot taken at (5, 1); the plot on the right shows the home vectors for a snapshot taken at (5, 6).

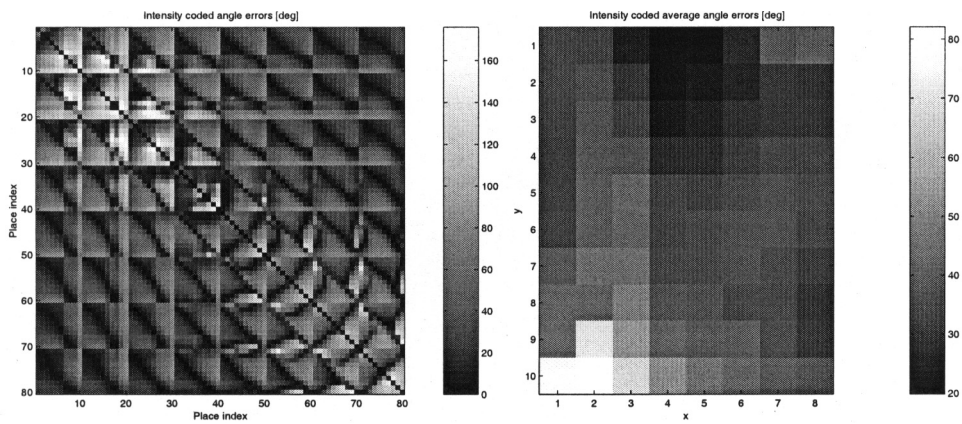

Figure 8 Left: Intensity-coded angle errors for all possible place pairs, averaged over 100 trials. Right: Intesity-coded average angle errors for each place in the room (80 grid positions) paired with all others, averaged over 100 trials.

monotonically during the homing task (Franz, Schölkopf, Mallott, & Bülthoff, 1998a). The home vector field after the Hebbian learning procedure has been plotted for two different snapshot positions (5, 1) and (5, 6) as shown in Figure 7.

In Figure 8 left, the intensity-coded angle errors for all possible place pairs are shown, averaged over 100 trials with different initial weights. The plot is symmetric, and one can clearly see that the angle errors are not equally distributed on all grid positions but are larger for certain place combinations. There is also a small area in the lower left part of the room with high angle errors on average (compare Figure 8 right).

4.2 Learning on the Mobile Robot

The performance in the real world during on-line learning has been tested both by recording the angle errors during exploration and by homing tasks. An example of the internal state of the mobile robot during exploration and homing is depicted in Figure 9. The neural network weights have adapted to the same structure as in the off-line experiments. As will be shown in Section 5.1, the learned visual homing algorithm is not dependent on any specific environment but is determined by intrinsic geometric properties. When each two snapshots have been recorded, the angle error between

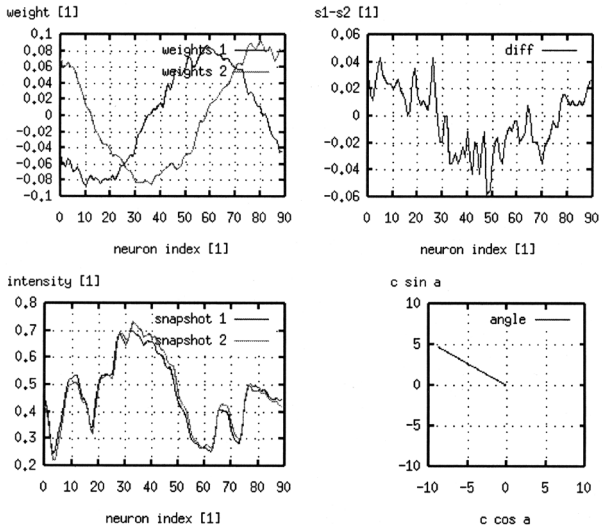

Figure 9 Internal and sensory state of the mobile robot during exploration (after the weights have converged to stable values). Top left: The current values of the weights. Bottom left: The intensity values of the two snapshots. Top right: The difference between those two snapshots. Bottom right: The compass direction α as obtained from the magnetic compass is displayed (in polar coordinates).

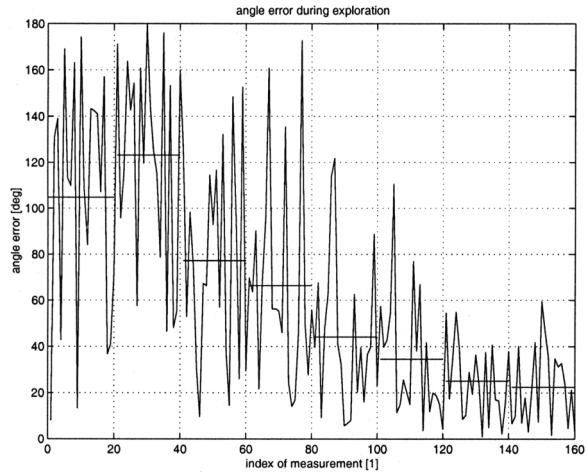

Figure 10 Angle error over time during the exploration and learning phase on the mobile robot. The angle error is the absolute angle included between the direction suggested by the neural network output (before adapting the weights with these specific snapshots) and the measured direction the mobile robot has taken between the two snapshot positions. The average angle errors over each 20 runs are shown as horizontal lines.

the measured compass direction and the vector produced by the neural network have been recorded before the two snapshots are used for the Hebbian learning. The initial learning rate was set to $\eta_0 = 0.04$ with $\eta_{t+1} = 0.999\eta_t$. One can clearly see in Figure 10 that the average angle error is decreasing during learning from values corresponding to random guesses of the homing vector to values below 90°. The average angle errors over each 20 runs are shown as horizontal lines. Learning on the mobile robot during exploration tours needs fewer learning steps than off-line learning with the recorded images, since only snapshot pairs with a direct connection (ca. 80 cm) between their positions are used as input to the neural network.

After exploration of the environment, the homing tasks are performed by driving the mobile robot manually to different positions within the room, allowing it to take a home snapshot, steering it away from this position by a distance of approximately 1–2 m and letting it perform homing as described in Section 3.4. The mobile robot reaches the goal in most of the combinations of goal and starting position, often approaching the goal position in a curve rather than a straight line. The observed homing behavior is comparable with the results obtained with the set of recorded images (See Figures 7 and 8) taken in the same room. Note that the general requirements for visual homing are that a certain portion of the landmarks is visible in both snapshots.

5 Discussion

5.1 Explanations for Learning and Homing

Having demonstrated learning of a visual homing strategy using Hebbian learning in a very simple neural network structure, we give some explanation of why this strategy is successful. In Figure 11, a schematic drawing of two snapshot positions with the corresponding one-dimensional omnidirectional snapshots is shown. Applying the isotropic as well as the equal distance assumption as introduced by Franz et al. (Franz et al., 1998a), the orientation of the translation vector d between the two snapshot positions can be determined from the snapshots.

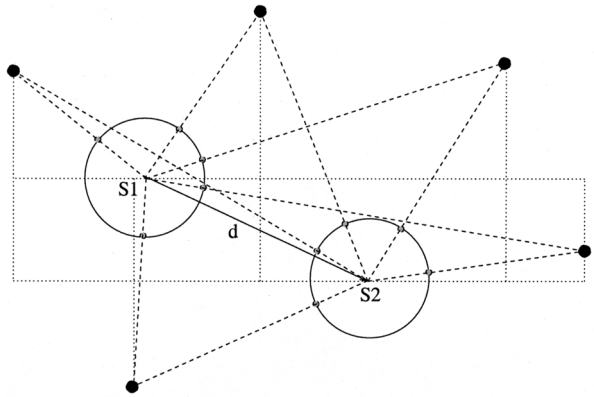

Figure 11 Schematic drawing of two snapshot positions with the corresponding one-dimensional omnidirectional snapshots. Applying the isotropic as well as the equal distance assumption as introduced by Franz et al. (Franz et al., 1998a), the orientation of the translation vector *d* between the two snapshot positions can be determined from the snapshots.

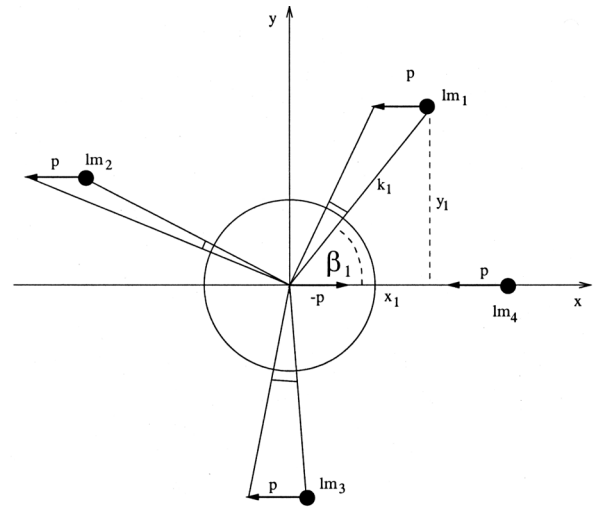

Figure 12 Schematic drawing of the visual field of the mobile robot during a translation $-p$, which is equivalent to the surrounding landmarks (lm) translating with p. The change in the angle β_i is dependent on sin β_i, v, and k_i.

Three rules can be generated from the intrinsic properties of the environment:

1. If both omnidirectional views are rotated by an angle α, the home vector is rotated by $-\alpha$.
2. If the two omnidirectional views are exchanged with each other, the home vector is rotated by π.
3. It follows: If the omnidirectional views are both rotated by π and exchanged, the home vector stays the same.

It has been shown by Hafner and Möller (2001) that, given these properties, the neural network weights need to have a sinusoidal structure, and that one snapshot has to be subtracted from the other. Here, the subtraction is already inherited in the neural network structure by using "excitatory" synapses from the home snapshot and "inhibitory" synapses from the other snapshot. Two open questions remain:

1. Why do the weights adapt to this structure using Hebbian learning?
2. Why is it possible to home with it?

The first question can be answered by looking at some properties of the subtracted snapshots. First, we consider a translatory movement with constant velocity v as depicted in Figure 12. A translation p of the mobile robot is equivalent to a translation $-p$ of the environment. To simplify the calculation, the coordinate system is defined in a way that $p_y = 0$ and $p_x = \|p\|$. We examine the change in the angle β_i for each landmark lm_i during the movement p. Please refer to the Appendix for the intermediate steps.

$$\frac{\mathrm{d}\beta_i}{\mathrm{d}t} = -\frac{\sin\beta_i}{k_i} v \tag{6}$$

The change in β_i is proportional to sin β_i, v, and $\frac{1}{k_i}$ where k_i is the distance to the landmark lm_i, and v is a constant velocity. The k_i are assumed to be constant on average over time. Since the snapshots are normalized and lowpass filtered, a small change in position on the sensor ring results in a small change in intensity at this position. The difference vector n of the two snapshots in the neural network corresponds to this change in intensity. Consequently, over several runs with different landmark configurations, we have a sine-shaped inhomogeneous distribution ρ_m of intensity on the difference n_j of the two one-dimensional omnidirectional snapshots (see Figure 13). ρ_m has a positive peak at position m with sin $\beta_m = 1$ and a negative peak at $(m + \frac{l}{2})$ mod l, where l is the number of neurons per snapshot. This distribution leads to an enhancement of the weights connecting n_j (j around m) with x and y during the Hebbian learning procedure.

Considering the rotation of the coordinate system by an angle α, the change in the synaptic weights is

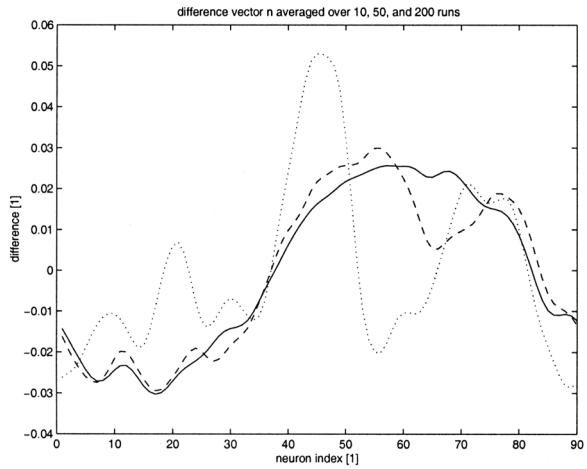

Figure 13 Difference vector $n = s1 - s2$ for a movement in the *x*-direction using the recorded images, averaged over 10 (dotted line), 50 (dashed line), and 200 (solid line) randomly chosen image pairs.

$\Delta w_{kx} = \eta n_k x(\alpha) = \eta n_k \cos\alpha$ (before normalization) with $k = \frac{\alpha l}{2\pi}$. The same holds for movements in the *y*-direction and any combinations, transforming the weight vectors w_x and w_y to sine-shaped curves with a phase shift of $\frac{\pi}{2}$.

The second question results in a comparison with an existing model: Homing is possible, since the learned model is directly comparable with the ALV model (Lambrinos et al., 2000), which allows for visual homing. The ALV model calculates the homing vector h by subtracting the AL vector at the target position from the AL vector at the current position:

$$h = \mathrm{ALV}_{\mathrm{cur}} - \mathrm{ALV}_{\mathrm{tar}},$$

where $\mathrm{ALV}_{\mathrm{tar}} = \Sigma_{i=1}^{n} \mathrm{lan}_i^{\mathrm{tar}}$ and $\mathrm{ALV}_{\mathrm{cur}} = \Sigma_{i=1}^{n} \mathrm{lan}_i^{\mathrm{cur}}$ with $\mathrm{lan}_i^{\mathrm{cur}}$ and $\mathrm{lan}_i^{\mathrm{tar}}$ being the landmark vectors.

The homing vector v_h of the neural network is calculated as (let l be the number of neurons per snapshot and $g_i = \frac{2\pi i}{l}$ with an index $i \in \{0, \ldots, l-1\}$):

$$\begin{aligned} v_h &= (x, y) \\ &= \left(\sum_{i=0}^{l-1} w_{ix} n_i, \sum_{i=0}^{l-1} w_{iy} n_i \right) \\ &= C \left(\sum_{i=0}^{l-1} \cos(g_i) n_i, \sum_{i=0}^{l-1} \sin(g_i) n_i \right) \\ &= C\mathrm{ALV}_n \\ &= C(\mathrm{ALV}_{s1} - \mathrm{ALV}_{s2}) \end{aligned}$$

Using lowpass-filtered intensity values for the snapshots without applying any additional filtering or landmark extraction, ALV_1 and ALV_2 represent the vector pointing toward the center of mass of the sensor ring rather than an average landmark vector.

5.2 Comparison with Existing Models

To the best of my knowledge, this article describes the first model of *learning and adaptation* of visual homing on a mobile robot using the snapshot hypothesis. As has been shown, the homing model resulting from the learning procedure is similar to the ALV model (Lambrinos et al., 2000). The main difference lies in the fact that we are not applying any landmark extraction as is necessary in the ALV model. Our learned model lies somewhere between a template model, such as the snapshot model (Cartwright and Collett, 1983), and a parameter model, such as the ALV model. The question of whether insects are using a template model for visual homing, like the snapshot model, or a parameter model, like the ALV model, or a mixture of both is still unresolved (Möller, 2001).

Lambrinos et al. (2000) have implemented a version of the snapshot model on the mobile robot "Sahabot" and have successfully tested it using artificial landmarks. The ALV model has been implemented in an analog version (Möller, 2000), being tested with black landmarks on a white background.

Another method that works with unsegmented grey value images is Franz et al.'s (1988a) homing model with parameterized displacement fields. This model is computationally more expensive, but it has the advantage that the views do not have to be aligned to a global compass orientation.

5.3 Future Work

The learned visual homing algorithm represents a general homing strategy that is independent of a specific environment as has been shown in theory and confirmed with experimental results. Future experiments have to be performed to investigate whether there are any minimal requirements for these environments, for example, whether outdoor environments need a special kind of image filtering.

Another area that needs further investigation is environments with obstacles. The ALV model comprises an emergent obstacle avoidance due to the

occlusion of remote landmarks by near landmarks. This behavior was also achieved by learned visual homing strategies in simulations (Hafner and Möller, 2001) but needs additional examination in real-world situations.

5.4 Conclusions

It has been shown both theoretically and with mobile robot experiments that learning of a visual homing strategy is possible using simple neural network structures together with Hebbian learning. The learning rule leads to an adaptation of the neural network weights during online exploration tours, resulting in a visual homing model similar to the ALV model, consequently strengthening the ALV hypothesis. In contrast to previous implementation of visual homing, no object recognition or landmark segmentation is required. The resulting homing strategy is widely independent of any special features of the environment.

It is suggested that only part of the visual homing abilities in animals is innate, for example, some basic neural structure. The navigation ability itself is acquired after birth through adaptation to the specific morphological properties of each animal. It has been shown in this article that such an adaptation is possible using Hebbian learning during small exploration tours. The neural connections can also be adapted to account for a change in the morphology as can happen during growth or as the result of an injury.

Acknowledgments

Many thanks to Ralf Möller and Fumiya Iida, and Lukas Lichtensteiger for helpful discussions and comments on the manuscript. This research has been supported by grant #20-61372.00 of the Swiss National Science Foundation.

References

Cartwright, B. A., & Collett, T. S. (1983). Landmark learning in bees. *Journal of Comparative Physiology*, *151*, 521–543.

Chahl, J. S., & Srinivasan, M. V. (1997). Reflective surfaces for panoramic imaging. *Applied Optics*, *36*, 8275–8285.

Collett, M., & Collett, T. S. (2000). How do insects use path integration for their navigation? *Biological Cybernetics 83*, 245–259.

Collett, T. S. (1992). Landmark learning and guidance in insects. *Philosophical Transactions of the Royal Society of London B, 337,* 295–303.

Franz, M. O., Schölkopf, B., Mallot, H. A., & Bülthoff, H. H. (1998a). Where did I take that snapshot? Scene-based homing by image matching. *Biological Cybernetics*, *79*, 191–202.

Franz, M. O., Schölkopf, B., Mallot, H. A., & Bülthoff, H. H. (1998b). Learning view graphs for robot navigation. *Autonomous Robots*, *5*, 111–125.

Georgopoulos, A. P., Schwartz, A.B., & Kettner, R. E. (1986). Neuronal population coding of movement direction. *Science*, *233*, 1416–1419.

Hafner, V. V., & Möller, R. (2001). Learning of visual navigation strategies. In M. Quay, P. Gaussier, & J. Wyatt, (Eds.), *Proceedings of the European Workshop on Learning Robots (EWLR-9)* (pp. 47–56).

Hebb, D. O. (1949). *The organization of behavior: A neuropsychological theory*. New York: Wiley.

Lambrinos, D., Maris, M., Kobayashi, H., Labhart, T., Pfeifer, R., & Wehner, R. (1997). An autonomous agent navigating with a polarized light compass. *Adaptive Behavior, 6*, 131–161.

Lambrinos, D., Möller, R., Labhart, T., Pfeifer, R., & Wehner, R. (2000). A mobile robot employing insect strategies for navigation. *Robotics and Autonomous Systems, 30*, 39–64.

Möller, R. (2000). Insect visual homing strategies in a robat with analog processing. *Biological Cybernetics, 83*, 231–243.

Möller, R. (2001). Do insects use templates or parameters for landmark navigation? *Journal of Theoretical Biology*, *210*(1), 33–45.

Morris, R. G. M. (1981). Spatial location does not require the presence of local cues. *Learning and Motivation*, *12*, 239–260.

Müller, M., & Wehner, R. (1994). The hidden spiral: Systematic search and path integration in desert ants, *Cataglyphis fortis*. *Journal of Comparative Physiology A, 175,* 525–530.

Oja, E. (1982). A simplified neuron model as a principal component analyzer. *Journal of Mathematical Biology*, *15*, 267–273.

Shors, T. J., & Matzel, L. D. (1997). Long-term potentiation: What's learning got to do with it? *Behavioral and Brain Sciences, 20*(4), 597–655.

Trullier, O., Wiener, S. I., Berthoz, A., & Meyer, J.-A. (1997). Biologically based artificial navigation systems: Review and prospects. *Progress in Neurobiology, 51*, 483–544.

Wehner, R. (2001). Polarization vision—a uniform sensory capacity? *Journal of Experimental Biology*, *204*, 2589–2596.

Zollikofer, C. P. E., Wehner, R., & Fukushi, T. (1995). Optical scaling in conspecific *Cataglyphis* ants. *Journal of Experimental Biology*, *198*, 1937–1646.

Appendix

We examine the change in the angle β_i for each landmark lm_i during the movement p with $p_y = 0$ and $p_x = \|p\|$ (see Figure 12):

$$\tan \beta_i = \frac{y_i}{x_i} \Rightarrow \beta_i = \arctan\left(\frac{y_i}{x_i}\right) \tag{A1}$$

$$\frac{\mathrm{d}\beta_i}{\mathrm{d}t} = \frac{\mathrm{d}\beta_i}{\mathrm{d}x}\frac{\mathrm{d}x}{\mathrm{d}t} + \frac{\mathrm{d}\beta_i}{\mathrm{d}y}\frac{\mathrm{d}x}{\mathrm{d}t} \tag{A2}$$

$$= \frac{\mathrm{d}\beta_i}{\mathrm{d}x} v \tag{A3}$$

$$= \frac{1}{1 + (\frac{y_i}{x_i})^2}\left(-\frac{y_i}{x_i^2}\right) v \tag{A4}$$

$$= \frac{-y_i}{x_i^2 + y_i^2 v} \tag{A5}$$

$$= \frac{-y_i}{k_i^2} v \tag{A6}$$

$$= -\frac{\sin\beta_i}{k_i} v \tag{A7}$$

The change in β_i is proportional to $\sin \beta_i$, v and $\frac{1}{k_i}$, where k_i is the distance to the landmark lm_i.

About the Author

Verena Vanessa Hafner is currently pursuing her Ph.D. at the Artificial Intelligence Laboratory, Department of Information Technologies, University of Zurich, Switzerland. She completed her undergraduate studies in mathematics and computer science in Germany, and received her M.Res. in computer science and artificial intelligence with distinction from COGS, University of Sussex, UK in 1999. Her primary research interest is neural computation and spatial cognition in the area of biorobotics, and in particular learning of animal and robot navigation strategies.